RSC Advances

ROYAL SOCIETY OF CHEMISTRY

www.rsc.org/advances

Blend film based on fish gelatine/curdlan for packaging applications: Spectral, microstructural and thermal characteristics

To be submitted to RSC Advances

Mehraj Ahmad [a*], Nilesh Prakash Nirmal [b], Julalak Chuprom [c]

[a] Institute of Nutrition (INMU), Mahidol University, 999 Phutthamonthon 4 Rd., Salaya, Nakhon Pathom 73170, Thailand

[b] Center for Nutrition and Food Sciences, University of Queensland, St. Lucia, Brisbane 4072, QLD, Australia

[c] Department of Microbiology, Faculty of Science, Prince of Songkla University, Hat Yai, Songkhla, 90112, Thailand

* To whom correspondence should be addressed. Tel: +66-2800-2380, Ext-296

Fax: +66-2441-9344, e-mail: mehraj.ahm@mahidol.ac.th

Abstract

A series of novel fish gelatine/curdlan (FG/CL) blend films at different ratios (FG/CL≈10:0, 8:2, 6:4, 5:5 and 0:10 %, w/w) were successfully fabricated at pH 12 via a casting approach, and their physico-mechanical, spectral, microstructural and thermal properties were investigated as a function of CL content. FG/CL blend films exhibited lower tensile strength (TS) but higher elongation at break (EAB) and water vapour permeability (WVP), compared to FG film (P<0.05). Increased contact angle (θ) and moisture content (MC), but decreased water solubility (WS) were obtained for FG/CL blend films having the higher proportion of CL (P<0.05). Furthermore, the addition of CL decreased a^*- (redness) and transparency values (P<0.05), but enhanced L^*- (lightness), b^*- (yellowness) and ΔE^*-values (total colour difference) (P<0.05) in FG/CL blend films. Light transmission in ultraviolet (UV) and visible regions (200-800 nm) was lowered in all FG/CL blend films, indicating excellent light barrier characteristics. Significant changes in molecular order and decreased intermolecular interactions in the matrix of FG/CL blend film were determined based on FTIR spectroscopy. TGA and DTG curves displayed that FG/CL (8:2) blend film had enhanced heat stability as evidenced by higher heat-stable mass residues (34.1 %, w/w), compared to FG film (26.6 %, w/w) in the temperature range of 50-600 °C. DSC thermogram suggested the solid-state morphology of FG/CL (8:2) blend film that consisted of amorphous/microcrystalline phase of partially miscible FG/CL aggregated junction zones and the coexisting of unbound CL domains. SEM micrographs elucidated that FG/CL (8:2) blend film was slightly rougher than FG film, but no signs of phase separation between film components were observed, thereby confirming its prospective use as food packaging material.

Keywords: Blend film; Fish gelatine; Curdlan; Thermo-mechanical properties

1. Introduction

The development of high performance, eco-friendly and biodegradable packaging materials is critically important to replace the conventional petrochemical-plastics which have obvious disadvantages especially environmental pollution and serious ecological problems. Fish gelatine and curdlan attracts the interest as biopolymers for packaging applications due to their excellent film-forming ability, relative abundance, non-toxicity, miscibility, biocompatibility and biodegradability. Fish gelatine (FG) is a natural hydrocolloid formed by the denaturation (proteolysis) of fibrous collagen present in the skin and bones generated as a waste during fish processing.[1] The transition of collagen to gelatine involves a process in which highly organised collagen fibres (water insoluble) is transformed from an infinite asymmetric network of linked tropocollagen units to a more depolymerised system of independent molecules called gelatine (water soluble).[2] FG is composed of proteins (85-92 %), minerals (3-7 %), and moisture (8-12 %).[2] Its molecular weight (MW) varies from 65 to 300 kDa and could be visualised as copolymer build-up from triads of α-amino acids with glycine at every third position (soft blocks) and triads of hydroxyproline, proline and glycine (rigid blocks).[3] All the polypeptide chains contain intrinsic hydrophilic as well as hydrophobic domains, which enable FG to be an ideal dispersing, coating and film-forming agent.[4] FG usually produce films and coatings with adequate physico-mechanical properties and excellent barrier characteristics against ultraviolet light (UV), gas, organic vapour and oil, compared to synthetic films at lower relative humidity.[2] Although, FG films have distinctive features, but the poor water barrier and water resistant efficiencies under high humid conditions, irregular mechanical properties and low melting temperature have limited their use in wide range of application.[4] Nevertheless, the films must have favourable and functional

characteristics such as colourless, odourless, hygienic, thermostable, low weight, high strength, and sufficient flexibility in order to be commercially viable. In addition to appropriate mechanical properties, the films must also have adequate permeability to moisture, aroma and gas. However, the specific barrier requirements of the films depend on products characteristics and the intended end-use application. Various attempts have been carried out to improve the properties of FG films. The inherited hydrophilic character of FG films was minimised using traditional high-cost chemical [5], enzymatic [6], γ-irradiations [7] and thermal treatments.[8] Nevertheless, blending of FG with other miscible biopolymers could be an alternative, economical and sustainable approach to overcome various limitations of FG films. The different biopolymers in a resulting blend film could play diverse roles and impart desirable attributes.[2] In general, the properties of blend films are influenced by the physical and chemical nature of biopolymers such as size distribution, biopolymer ratio, volume fraction, conformations and hydration behaviours, and the intrinsic adhesion with the biopolymer surface.[2,4] Biopolymers with the suitable functional group are preferred material for the fabrication of high performance films.[9] The formation and development of stronger interfacial interaction offers to categorise the composites into rigid materials.[10]

Curdlan (CL) is an extracellular bacterial polysaccharide, produced by the non-pathogenic and non-toxicogenic members of *Rhizobiaceae* (*Agrobacterium* sp.) via fermentation in the form of triple-stranded helical aggregates.[11] Its linear glucan structure is composed of (1–3)-β-D-glucosidic linked glucose residues.[12] It is insoluble in water, alcohol or acid solution, but could be solubilised in alkaline solutions (pH≥12) such as sodium hydroxide and trisodium phosphate.[13] CL is white powder with high fluidity and pseudo-crystallinity.[13] Although CL is insoluble in

water, but it still forms smooth sheet layers indicating an intriguing two-dimensional (2D) network of gel in frozen state.[14] CL also possesses unique property of forming heat-induced three-dimensional (3D) elastic gels in aqueous suspension with distinct thermal stabilities determined by the heat-treatment.[14] Low-set thermo-reversible and high-set thermo-irreversible (optically transparent) gels are typically prepared when an aqueous dispersion is heated between 55-80 °C and >80 °C, respectively.[15] In low-set gel, there is cross-linking between CL micelles, which are occupied by molecules of a single-helix through hydrogen bonds, whereas, in the high-set gel, the CL micelles are cross-linked by a triple-stranded helix through hydrophobic interactions.[16] Due to its water insoluble and thermo-gelable properties, CL could be used to improve a water barrier capability and thermal stability of FG films. CL was used as a drug delivery carrier due to its gelation property[17]; and it is also known for anti-HIV[18] and anti-tumour activities.[19] CL was approved by the Food and Drug Administration (FDA) as a food additive (formulation aid, processing aid, stabiliser and thickener, or texturiser).[20]

To the best of our knowledge, there is no information regarding the preparation of blend films from FG and CL containing glycerol as plasticiser. Thus, combining the unique collective properties of both biopolymers, the fabrication of FG/CL blend films via casting method is of great interest. Therefore, the objective of this investigation was to prepare blend films at different FG/CL ratios, and to evaluate their properties as a function of blend composition and pH.

2. Materials and methods

2.1. Materials

Type B commercial fish gelatine (FG) extracted from tilapia skin (~240 bloom strength, pI~5.0) containing 85.7 % (w/w) of protein as determined by the Kjeldhal

method (AOAC)[21], was purchased from Lapi Gelatine S.p.a (Empoli, Firenze, Italy). Curdlan (CL; DP~450) was purchased from Wako Chemical USA, Inc. (Richmond, Virginia, USA). Sodium azide was obtained from Sigma Chemical Co. (St. Louis, MO, USA). Glycerol (98 % purity) and sodium hydroxide (NaOH) were procured from Merck (Merck Chemicals, Darmstadt, Germany). All chemicals used in this study were of analytical grade.

2.2. Fabrication of fish gelatine/curldlan blend films (FG/CL)

Prior to fabricating FG/CL blend films, FG was dissolved in distilled water to obtain the protein concentration of 2 % (w/v), followed by heating at 60 ºC for 30 min using a hot plate magnetic stirrer (IKA® C-MAG HS-7, Selangor, Malaysia). After dissolution, the FG solution was adjusted to pH 12 with 1 M NaOH solution. Thereafter, glycerol at 30 % (w/w) based on protein content was added as plasticiser and the mixture was gently stirred for 30 min at room temperature. Similarly, CL was solubilised in distilled water with continuous stirring to obtain the final concentration of 2 % (w/v). The CL suspension was adjusted to pH 12 using 6 N NaOH to ensure complete disintegration of CL granules and formation of a homogeneous dispersion. The resulting dispersion was added with glycerol at 30 % (w/w) based on CL content and left stirring overnight at ambient temperature. Subsequently, blend film-forming solutions (FFSs) were prepared by mixing the above solutions at different FG/CL ratios (10:0, 8:2, 6:4, 5:5 and 0:10 %, w/w). The blend FFSs were homogenised at a speed of 11,000 rpm for 2 min using a homogeniser (Model T25 basic, IKA®18, 19 Labortechnik, Selangor, Malaysia). Prior to film casting, the viscous FFSs were degassed for 10 min using ultra-sonicator water bath (Elmasonic EH075EL, New Jersey, USA) until homogenous solution was obtained. To study the effects of pH, additional film was also prepared from FG at pH 7.0.

2.3. Film casting, drying and conditioning of films

FFSs (4.0±0.0 g) were cast onto a rimmed silicone resin plate (5 × 5 cm^2), air-blown for 12 h at room temperature, followed by drying in an environmental chamber (Binder, KBF 115 # 00-19735, D-78532, Tuttalingen, Germany) at 25±0.5 °C and 50±5 % RH for 24 h. Dried films were manually peeled off and subjected to further analyses.

Prior to testing, films were conditioned for 48 h at ~50±5 % relative humidity (RH) and 25±0.5 °C. For ATR-FTIR, DSC, TGA and SEM studies, films were conditioned in a desiccator containing dried silica gel for 1 week to minimise the plasticising effect of water, followed by drying in a desiccator containing P_2O_5 gel for 2 weeks at room temperature (28-30 °C) to obtain the most dehydrated films (≤5 moisture content).

2.4. Analyses

2.4.1. Thickness

The thickness of films was measured using a digital electronic micrometer (Model ID-C112PM, Serial No. 00320, Mituyoto Corp., Kawasaki-shi, Japan). Ten random locations around each film sample were used for determination of thickness. Mean thickness values for each sample were taken and used in the calculation of WVP and TS.

2.4.2. Measurement of stress-strain properties

The stress-strain properties, such as tensile strength (TS), Young's modulus (E) and elongation at break (EAB) of films were determined based on ASTM method (American Society for Testing and Materials) as described by Iwata et al.[22] The test was performed using the Universal Testing Machine (Lloyd Instrument, Hampshire, UK) in the controlled room at 25-28 °C and ~50±5 % RH. Ten films (2 × 5 cm^2) with

the initial grip length of 3 cm were used for testing. The films were clamped and deformed under tensile loading using a 100 N load cell with the cross-head speed of 30 mm/min until the samples were broken. The TS was expressed in MPa and calculated by:

$$\text{TS (MPa)} = \frac{P\max}{A} \qquad \text{Eq. (1)}$$

where P_{max} is the maximum force (N) necessary to pull the sample apart, and A is the initial cross-sectional area of the sample film (m^2) determined by multiplying the film width by the film thickness.

Percentage elongation at break is the amount of uniaxial strain at fracture and was calculated by:

$$\text{EAB (\%)} = \frac{lb - lo}{lo} \times 100 \qquad \text{Eq. (2)}$$

where l_b is the film elongation at the moment of failure and l_o is the initial grip length (3. cm) of samples multiplied by 100.

Young's modulus of elasticity was expressed in MPa and was determined by calculating the slope of the elastic (linear) region of an engineering stress-strain curve:

$$\text{E (MPa)} = \frac{\Delta S}{\Delta e} \qquad \text{Eq. (3)}$$

where ΔS is the change in tensile stress and Δe is the change in tensile strain over the elastic region.

2.4.3. Water vapour permeability (WVP)

WVP was measured using gravimetric modified cup method based on ASTM method as described by Shiku et al.[23] Briefly, films were sealed on an aluminium permeation cup containing dried silica gel (0 % RH) with silicone vacuum grease and rubber gasket, and held with four screws around the cup's circumference. After

measuring the initial weight, test cups were placed in a desiccator containing the distilled water (30 ºC, ~50±2 % RH). Consequently, test cups were weighed to the nearest 0.0001 g with an electronic balance (Model CPA225D, Sartorious Corp., Goettingen, Germany) at 1 h intervals over an 8 h period. A plot of weight gained versus time was used to determine the WVP and the slope of the linear portion of this plot represented the steady state amount of water vapour diffusing through the film per unit of time (g/h). Five films were used for analysis and WVP of the film was calculated as follows:

$$\text{WVP (g m}^{-1}\text{ s}^{-1}\text{ Pa}^{-1}) = wlA^{-1}\,t^{-1}\,(P_2 - P_1)^{-1} \qquad \text{Eq. (4)}$$

where w is the weight gain of the cup (g); l is the film thickness (m); A is the exposed area of film (m^2); t is the time of gain (s); (P_2 - P_1) is the vapour pressure difference across the film (4,244.9 Pa at 30 °C).

2.4.4. Moisture content and solubility

Three samples of each film were weighed (m_w) and subsequently dried in an air-circulating oven at 105 °C for 48 h. Films were then reweighed (m_0), to determine their moisture content (MC):

$$\text{MC (\%)} = \frac{mw - mo}{mw} \times 100 \qquad \text{Eq. (5)}$$

Solubility of films in water was determined as the content of dry matter matter solubilised after 24 h of immersion in water according to the modified method of Gennadios et al.[24] Two pieces of conditioned films (3 × 2 cm^2) previously dried until constant weight, were immersed in 10 mL of distilled water containing 0.1 % (w/v) sodium azide in 50 mL screw cap tubes. The tubes were capped, placed in a shaking water bath (Model UNIMAX 1010, Heidolph Instruments GmbH & Co.KG, Schwabach, Germany) and mixtures were shaken continuously at room temperature for 24 h. The undissolved debris was obtained after centrifugation at 3000 ×g for 10

min at 25 ºC using centrifuge (Model Allegra 25R Centrifuge, Beckman Coulter, Krefeld, Germany). The pellets were dried until constant weight in an oven at 105 ºC to obtain the dry unsolubilised film matter. The weight of solubilised dry matter was calculated by subtracting the weight of unsolubilised dry matter from the initial weight of dry matter and expressed as the percentage of total weight.

2.4.5. Colour properties

Colour of films was determined using a CIE colourimeter (Hunter associates laboratory Inc., Reston, VA, USA). Colour of films was expressed as L^*- (lightness/brightness), a^*- (redness/greenness) and b^*- (yellowness/blueness) values. Total difference in colour (ΔE^*) was calculated according to the following equation [25]:

$$\Delta E^* = \sqrt{(\Delta L^*)^2 + (\Delta a^*)^2 + (\Delta b^*)^2} \quad \text{Eq. (6)}$$

where ΔL^*, Δa^* and Δb^* are the differences between the corresponding colour parameter of the sample and that of white standard ($L^* = 93.6$, $a^* = -0.9$ and $b^* = 0.4$).

2.4.6. Light transmission and transparency

Light transmission of films against ultraviolet (UV) and visible light were measured at selected wavelengths between 200 and 600 nm, using a UV-Visible spectrophotometer (Model UV-1800 Shimadzu, Kyoto, Japan) according to the method of Jongiareonrak et al.[26] The transparency value of film was calculated by the following equation[27]:

$$\text{Transparency value} = (-\log T_{600})/x \quad \text{Eq. (7)}$$

where T_{600} is the fractional transmittance at 600 nm and x is the film thickness (mm). The higher transparency value represents the lower transparency of films.

2.4.7. Contact angle measurement

Contact angle (θ) of films (pH 12) was measured in a conditioned room (25 °C) by the sessile drop method using contact angle meter (Model KSV CAM 101,

KSV Instruments, Ltd., Helsinki, Finland), equipped with image analysis software. Briefly, film sample (2 × 2 cm^2) was placed on a movable platform and levelled horizontally. A droplet of ultra-pure water (30 µL) was placed on a film surface using 500 µL microsyringe (Hamilton Robotics Inc., Bonaduz, GR, Switzerland) attached with a needle of 0.75 mm diameter. Image analyses were carried out using image recorder CAM 200 software and the contact angles were noted.

2.5. Characterisation of selected films

Amongst the various blend films, FG/CL (8:2) blend film showed the sufficient mechanical properties and was further subjected for characterisation, in comparison with FG and CL films.

2.5.1. Attenuated total reflectance-Fourier transforms infrared spectroscopy (ATR-FTIR)

FTIR spectra of selected films were determined using a FTIR spectrometer (Model Equinox 55, Bruker Co., Ettlingen, Germany) equipped with a horizontal ATR Trough plate crystal cell (45º ZnSe; 80 mm long, 10 mm wide and 4 mm thick) (PIKE Technology Inc., Madison, WI, USA) at 25 ºC. Films were placed onto the crystal cells and the cells were clamped into the mount of FTIR spectrometer. The spectra in the range of 650-4000 cm^{-1} with automatic signal gain were collected in 32 scans at a resolution of 4 cm^{-1} and were ratioed against a background spectrum recorded from the clean empty cell at 25 ºC. Analysis of spectral data was carried out using the OPUS 3.0 data collection software programme (Bruker, Ettlingen, Germany). Prior to data analysis, the spectra were baseline corrected and normalised.

2.5.2. Differential scanning calorimetry

Thermal properties of selected films were determined using differential scanning calorimeter (Model DSC-7, Perkin Elmer, Norwalk, CT, USA). Temperature

calibration was performed using the indium thermogram. The films (4-5 mg) were accurately weighed into aluminium pans, hermetically sealed and scanned over the temperature range of -50-220 °C (1st heating scans) and -50-340 °C (2nd heating scans) with a heating rate of 10 °C/min. The dry ice was used as a cooling medium and the system was equilibrated at -50 °C for 5 min prior to the scan. The empty aluminium pan was used as a reference. The glass transition temperature (T_g) was calculated as the inflexion point of the base line, caused by the discontinuity of the specific heat of the sample. The maximum transition temperature (T_{max}) was estimated from the endothermic peak of DSC thermogram and transition enthalpy (ΔH) was determined from the area under the endothermic peak. All these properties were calculated with help of the DSC-7 software.

2.5.3. Thermo-gravimetric analysis (TGA)

Dried selected films were scanned using a thermo-gravimetric analyser (Model TGA-7, Perkin Elmer, Norwalk, CT, USA) from 40 to 600 ºC at a rate of 10 ºC/min.[28] Nitrogen was used as the purge gas at a flow rate of 20 mL/min. The percent weight loss (%) versus temperature plots were taken for thermo-gravimetric analysis (TGA) and derivative weight loss against temperature was taken for differential thermo-gravimetric analysis (DTG).

2.5.4. Microstructure

Microstructure of upper surface and cryo-fractured cross-section of the selected films was visualised using a scanning electron microscope (Model JSM-5800 LV, JEOL, Tokyo, Japan) at an accelerating voltage of 10 kV. The films were cryo-fractured by immersion in liquid nitrogen. Prior to visualisation, the films were mounted on brass stub and sputtered with gold in order to make the sample conductive, and photographs were taken at 8000× magnification for surface. For

cross-section, cryo-fractured films were mounted around stubs perpendicularly using double sided adhesive tape, coated with gold and observed at the 5000× magnification.

2.6. Statistical analyses

Experiments were performed in triplicate (n=3) with three different lots of film samples and a completely randomised design (CRD) was used. Data were presented as means ± standard deviation and a probability value of <0.05 was considered significant. Analysis of variance (ANOVA) was performed and the mean comparisons were done by Duncan's multiple range tests. Statistical analysis was performed using the Statistical Package for Social Sciences (SPSS for Windows, SPSS Inc., Chicago, IL, USA).

3. Results and discussion

3.1. Mechanical properties

Tensile strength (TS), Young's modulus (E) and elongation at break (EAB) of blend films prepared at different FG/CL ratios are summarised in Table 1. The maximum stress that the film can withstand while being stretched or pulled before failing or breaking is known as TS. E is the measure of intrinsic film stiffness or rigidity. FG film regardless of pH had the highest TS and E ($P<0.05$), compared with FG/CL blend films. This indicated that the FG film was more rigid and less extensible than the FG/CL blend films. As the level of CL increased, lower TS and E were observed in resulting blends films ($P<0.05$). This was plausibly governed by the structural change of the original gelatine network in the presence of CL network. Therefore, a greater dispersed CL content lowers the cohesion forces and the film resistance to break. The apparent plasticising effect produced by the addition of CL weakens the chain-chain interactions and promotes chain mobility in FG/CL blend

films. As a consequence, the polymer matrix is more flexible and the polymer chains can slide past each other more readily during tensile deformation. Nevertheless, no significant difference in TS was noted between FG/CL (6:4) and FG/CL (5:5) blend films (P>0.05). At pH 12, TS and E of FG/CL blend films were in the range of 6.7±1.5-20.5±1.3 MPa and 153.8±1.0-496.7±2.0 MPa, respectively. It was postulated that pH 12 (alkaline) of FFS yielded more negative charge in FG/CL blend, leading to higher repulsion among polymer chains as evidenced by lower TS and E.[29] Additionally, the more negatively charged CL molecules tend to aggregate to a greater extent, leading to less effective interfacial interaction with FG.[30] As a result, the force transfer at FG/CL interface was less effective, thus exhibiting less reinforcing effect. Nevertheless, E of CL film was higher than the FG/CL blend (6:4) and (5:5) films (P<0.05). FG film prepared at pH 7 (neutral) had highest TS and E due to enhanced intermolecular interaction among fibrous gelatine molecules. Generally, electrostatic repulsion between polymeric molecules at pH values beyond the isoelectric point (pI) could impede the intermolecular interaction between polymeric chains, thereby lowering the strength of film network. The extreme alkaline pH favoured the solubilisation and subsequent alignment of extended or stretched FG/CL molecules, in the way which less inter-junctions with weak interfacial bonds were formed between FG and CL matrix.[29] In case of CL film, lower TS (9.6±1.3 MPa) and E (235.3±1.9 MPa) was also noticed in comparison with FG film (P<0.05). This could be due to the transition of helical (ordered) form to the random coil (disordered) form under alkaline conditions.[31] Usually, heterogeneously aggregated/coiled structure consisting of hydrophilic surface and hydrophobic core occur in CL at acidic pH.[31]

EAB expresses the capability of a film to resist changes of shape without crack formation. Amongst all films added with CL, highest EAB accompanied with lower

TS was found in FG/CL (5:5) blend film (P<0.05). Increased CL content produced flexible FG/CL blend films as evidenced by higher EAB (P<0.05) due to the presence of weaker bonds (dipole-dipole interaction, London dispersion force and hydrogen bonding) stabilising the film matrix. At pH 12, EAB values of FG/CL blend films ranged from 21.8±1.8 to 41.3±4.8 %, which were significantly higher than FG film (14.7±3.3 %) and CL film (15.3±3.6 %) (P<0.05). At pH 7, FG film showed the lowest EAB value (P<0.05). Among all films, FG/CL (6:4) and FG/CL (5:5) blend films showed the highest EAB (P<0.05), in which EAB was increased by 160.3 and 181.1 %, respectively, compared with FG film (pH 12). This indicated the formation of ductile and stretchy FG/CL blend films by the incorporation of CL. In addition, glycerol added as a plasticiser acts by breaking polymer-polymer interactions (like hydrogen bonds and Van der Waals forces) and forming secondary bonds with polymer chains (bridging agent).[32] This phenomenon causes the adjacent chains to move apart thereby reducing film rigidity and increasing flexibility. Nevertheless, the adequate TS and EAB of FG/CL (8:2) blend film compared to FG film (pH 12), could be used for packaging applications at industrial scale. This blend film could absorb the normal stress encountered during its application, subsequent shipping and food handling. The interaction between biopolymers and other additives including water and plasticisers plays an important role in TS and EAB of packaging films.[33] The mechanical properties of films are largely associated with nature and the chemical structure of film forming materials, distribution and density of intra- and intermolecular interactions, which depend on the arrangements, and orientation of polymer chains in the network.[34] Thus, it was apparent that the strength, stiffness and flexibility of the blend films could be modified by changing the ratio of FG and CL.

3.2. Water vapour permeability (WVP)

WVP of blend films prepared at different FG/CL ratios is shown Table 1. The permeation of a given molecule through a polymeric matrix is a thermodynamic process that results from three combined mechanisms: absorption of the molecule at the polymeric surface, diffusion throughout the material and finally, desorption of the molecule from the surface. At pH 12, WVP of FG/CL blend films ranged from 4.7±0.6 to 7.8±0.8 ($\times 10^{-10}$ $gs^{-1}m^{-1}Pa^{-1}$), compared to FG film ($3.0\pm0.0 \times 10^{-10}$ $gs^{-1}m^{-1}Pa^{-1}$) ($P<0.05$). At pH 12, FG film and FG/CL blend films had relatively higher WVP values, compared with FG film (pH 7). Higher WVP of FG/CL blend films was coincidental with the lower TS and E of film (Table 1). At pH 12, FG/CL components of blend films were characterised by an emphatic hydrophilicity, which trigger hydrodynamic film-water interactions, enhancing sorption and permeability of water through the film. In addition, the lower intermolecular interactions due to electrostatic repulsion between negatively charged FG/CL molecules could not provide strong film network which plausibly led to the increased interstitial space between different polymeric chains of film matrix, with the subsequent increase in WVP. It was also postulated that the rigid and linear structure of CL molecules might be incompatible with FG chains as compared to the flexible and branched polymers. This resulted in phase separation due in part to less favourable interfacial interactions amongst different polymer segments and eventually facilitated the migration of water vapour through the films. Thus, the structuring of polymer inside the film matrix could significantly affect the WVP. Furthermore, CL promotes water clustering by competing with water at the active sites of the polymer matrix and forming micro cavities in the polymer network structure. The water is absorbed into the film matrix, leading to a less dense structure where chain ends are more mobile and increasing the transmission rate. In general, the water diffusion through films is governed by film

network.[35] Films with the compact and denser structure could lower the WVP more effectively than those with less compactness.[2] Nevertheless, no significant difference in WVP values was noted among FG/CL blend films regardless of CL content (P>0.05). Apart from that, polysaccharides possess higher water holding capacity than proteins, the affinity for water molecules will be greater in these films and therefore resulting in higher water diffusion forming films with higher WVP.[2] In the present study, the addition of CL in film matrix probably led to formation of disordered network with less compactness and thus could not prevent the diffusion of water vapour more effectively. Souza et al.[36] reported that the WVP of polymeric films depended on many factors, including solubility coefficient, integrity of film matrix, hydrophobicity, diffusion rate, ratio between crystalline and amorphous zones, thickness, polymeric chain mobility, and interactions between the functional groups of polymers.

3.3. Thickness

Thickness values of blend films prepared at different FG/CL ratios are shown in Table 1. FG film (control) had the smallest thickness value (20.0±3.0 μm) but FG/CL blend film showed the higher thickness values ranging from 27.0±1.0 to 46.0±2.0 μm (P<0.05); whereas, the thickness value of CL film was 32.0±4.0 μm. There was no significant difference noted in thickness between FG film prepared at pH 7 and pH 12 (P>0.05). Highest thickness value was noted in FG/CL (5:5) blend film (P<0.05) as a function of increased CL content (P<0.05). Increased thickness of FG/CL blend films could be plausibly due to the formation of protruded structures. The protruded structures consisted of coagulated polymeric chains in FG/CL blend films. Increased thickness of FG/CL blend films could also be correlated to the higher viscosity of CL which distends to large extent upon drying. Furthermore, CL addition

enhanced the development of heterogeneous film matrix, where FG and CL chains could not form the compact and ordered film network as evidenced by the increased thickness. In FG film matrix, the higher degree of compactness and ordered network was formed in which peptide chains align themselves with less protrusion as indicated by the lowest thickness. Moreover, the interactions between different polymeric chains in FG/CL blend films promoted a change in bulk which retained more water in film structure especially in protruded structure resulting in increased thickness. In general, film thickness depends on the composition of the FFS, viscosity and the nature of its components.[35] The film components also affect the alignment, sorting and compacting of the molecules during film drying process, thereby causing the differences in thickness.[4] The thickness of a film has a strong influence on the WVP. According to Park and Chinnan[37], the hydrophilic films show positive relationship between the thickness and permeability due to the interaction of water with the polymer matrix that occurs due to the structural changes caused by the swelling of the hydrophilic matrix. This affects the film structure and cause internal tensions that influence the permeation. Nevertheless, non-significant increase in WVP (P>0.05) was noted with the increased thickness in FG/CL blend films (Table 1)

3.4. Moisture content and solubility

Moisture content (MC) and solubility of blend films prepared at different FG/CL ratios are shown in Table 2. Based on the results, MC of FG/CL blend increased significantly with the increase in CL content (P<0.05). Amongst all films, highest MC was noted in FG/CL (5:5) blend film (P<0.05). The MC of all FG/CL blend films ranged from 19.5±0.8 to 25.1±0.2 %. Increased MC was coincidental with the significant decrease in TS and E of all FG/CL blend films (P<0.05) (Table 1). The highest solubility was noted in FG film prepared at pH 7 (94.9±0.2 %) and pH 12

(94.4±0.5 %), whilst FG/CL blend films exhibited lower solubility ranging from 63.9±0.8 to 67.9±0.8 %. Amongst all blend films, FG/CL (8:2) had the lowest solubility (63.9±0.8 %) in water (P<0.05). The result suggested that FG/CL ratio of 8:2 might yield the film matrix, which could trap glycerol efficiently. As a consequence glycerol could not be leached out with ease. Increased solubility of FG/CL (6:4) and FG/CL (5:5) blend films was observed. It has been reported that the solubility of plasticised film is in part due to leaching out of plasticiser (glycerol) in water.[4] For FG film, it was reported that polymeric molecules of FG are composed of hydrophilic amino acids and could be hydrated in the presence of water, leading to the ease of solubilisation.[4] The dissolution of water soluble FG involves the penetration of water to the polymer bulk and swelling. This is followed by disruption of hydrogen and van der Waals forces between polymer chains. FG/CL blend films displayed significant decrease in solubility as a function of increased CL content (P<0.05). It might be due to decrease in relative amount of FG, a highly water soluble protein, in the blend film. The lower solubility of FG/CL blend films might be due to the enhanced structural integrity and water resistance of FG/CL blend films provided by the water insoluble polymeric chains of CL.[2,17] Moreover, the decrease in solubility of FG/CL blend film could be linked to interaction between these two polymers in the film matrix, resulting in the lower hydrophilic sites available for absorbing water.[2,4] These intermolecular interactions might provide resistance and stability to the FG/CL blend films. Nevertheless, lowest solubility of CL film might be due to poor solubility of CL in aqueous solution, but the film could be hydrated in the presence of alkaline solution, leading to the ease of solubilisation. Although lower solubility of films is required during storage, but higher solubility of film could be advantageous during cooking food products coated with edible films.[38] The intermolecular interactions

could improve the cohesiveness of biopolymer matrix and decreased water sensitivity.[39] Film solubility can be viewed as a measure of the water resistance and integrity of a film.[40] Ahmad et al.[2] found a reduction of about ≥40 % (w/v) water solubility of plasticised fish gelatine film as a result of rice flour addition. However, increased film solubility could be related to water diffusion, ionisation of −OH and −COOH groups, polymer relaxation and dissociation of hydrogen and ionic bonds.[41] Thus, the incorporation of CL affected the solubility of resulting FG/CL blend films.

3.5. Colour

Colour parameters of blend films prepared at different FG/CL ratios are shown in Table 2. There was no significant difference noted in all colour parameter between FG film prepared at pH 7 and pH 12 (P>0.05). However, colour of FG/CL blend films was affected by the addition of CL in film formulations. The increased b^*-values (yellowness) with the coincidental decreases in a^*-values (redness/greenness) were found in FG/CL blend films, compared to the FG film (P<0.05). Amongst all the films, FG/CL (5:5) rendered the film with higher b^*- value (P<0.05). Nevertheless, there was no significant difference in b^*-value between FG/CL (8:2) and FG/CL (6:4) blend films (P>0.05). This indicated that the FG/CL blend films became more yellowish when the 50 % CL was added in the blend. Furthermore, the increased yellowness in FG/CL blend films occurred during the casting and drying process via Maillard reaction between amine groups of FG and carbonyl groups of CL as evidenced by the increased yellowness (b^*-values).[42] L^*- (lightness) and ΔE^*-values (total colour difference) of FG/CL blend films were not much different from that of the FG film. From the results, FG and CL films showed the highest a^*-values, compared to FG/CL blend films (P<0.05). The b^*-value of CL film was associated with the yellowish colouration due to the presence of (1–3)-β-D-glucosidic linked

glucose residues.[43] As the CL content increased, the yellowish colour did so as well (as measured by increased b^*-values) and the films were clearer (indicated by increased L^*-values). It was noticed that the decreases in a^*-values with coincidental increases in b^*-values were obtained as higher amount of CL was incorporated. There was no substantial change noticed in ΔE^*-values with the addition of CL in FG/CL blend films. Such changes in colour properties of resulting blend films were most likely attributed to the colouring components formed during the Maillard reaction. Therefore, film components had influence on the colour properties of resulting films, depending on the type, nature and concentration of biopolymer incorporated.[2,4] Generally, film colour can be an important factor in terms of consumer acceptance in packaging applications.

3.6. Light transmission and transparency

Transmission of UV and visible light at selected wavelength in the range of 200-800 nm of blend films prepared at different FG/CL ratios is shown in Table 3. At pH 12, light transmission of FG/CL blend films in UV region (200-280 nm) decreased when the CL content increased in the film formulation ($P<0.05$), compared with both FG films prepared at pH 7 and pH 12. Nevertheless, slight increase in light transmission (58.6-81.0 %) was noted in FG/CL (6:4) blend film in the visible range (350-800 nm) in comparison with FG/CL (8:2) and FG/CL (5:5) blend films. This increased light transmission of FG/CL (6:4) blend film was most likely governed by the arrangement or alignment of polymeric chains in film network. Besides, non-uniformities in the composition of the material could cause significant changes in light transmission.[2] FG/CL blend films had lowest transmission (20.1-31.4 nm) in UV region at 280 nm. This could be due to the cumulative effect produced by the CL molecules that absorb light at the wavelength below 300 nm. In addition, the aromatic

amino acids (Tyr, 0.8±0.0; Phe, 0.5±0.0 and Trp, 1.8±0.0) are well known sensitive chromophores of FG that typically absorb the UV light.[44] The films containing high aromatic amino acid content play an important role in UV barrier properties.[35] In general, FG/CL blend films showed remarkable barrier property to UV light, compared to FG film. The results suggested that the potential preventive effect of all FG/CL blend films on the retardation of product oxidation induced by UV light. The linear chain of glucose units held by glycosidic bonds in CL structure could absorb the energy of incoming light.[2] Besides, the lowered transmission in FG/CL blend films in both UV and visible range was correlated with the increased b^*-values, compared to FG film (P<0.05). The result suggested that CL added at higher amount had high light transmission barrier in both UV and visible ranges. Thus, light transmission more likely depended on the distribution of CL in the film matrix as well as their interaction with FG. This led to the differences in film matrix morphology with different light transmission. Thus, FG/CL blend films acquired the ability to protect packaged products against light, thus potentially could improve the shelf life and quality of food. Optical properties of films are an important attribute which influences its appearance, marketability, and their suitability for various applications.[4] Clear edible films are typically desirable with higher applicability and acceptability in food packaging systems.

From the results, FG film prepared at pH 7 had significantly higher transparency values than FG film prepared at pH 12. Higher transparency values indicated that the films had lower transparency. FG/CL blend films were more transparent when the CL was incorporated, as compared to FG film (P<0.05). This was evidenced by lower transparency values in FG/CL blend films as a function of increased CL content (P<0.05). Higher transparency might be associated with greater

film homogeneity. The higher transparency of FG/CL blend films could be deduced from the changes in the TS and EAB values. However, the clear and transparent nature of CL solution contributed to the enhanced transparency of resulting FG/CL blend films to some extent. The FG/CL blend films with strong UV prevention capacity without sacrificing transparency are expected to be used as a UV screening food packaging material.

3.7. Contact angle measurement

Fig.1. showed the contact angle values (θ) of blend films prepared at different FG/CL ratios (pH 12). From the results, contact angle values of blend films ranged from 91.9° to 95.4°, indicating that lower surface wettability with the addition of CL. Generally, films with higher contact angle value (θ≥90°) exhibited lower surface wettability, whereas biopolymer films with lower contact angle value (θ≤90°) showed high surface wettability. [45] As it is shown in Fig.1, contact angle values of FG and CL films were 88.6° and 92.0°, respectively. The contact angle of the FG/CL blend films increased concomitantly with the addition of CL. The surface wettability of blend films were in the following order: FG/CL (8:2) > FG (6:4) > FG/CL (5:5). These results showed that the surfaces of FG/CL blend films became more non-polar after the addition of CL. However, all the constituents in the blend, i.e., the FG and CL, have hydrophilic ionic groups and no hydrophobic surface. Thus, the observed increase in the contact angle of the FG/CL blend could be explained in terms of surface roughness and intermolecular interactions between polymer chains of the film matrix. This behavior indicates that FG/CL interactions promoted the change not only in the density but also in the structure that allowed less water to get attracted with the film surface. This could be further explained by conformational changes in which non polar groups tend to be oriented towards the air-film interface and thus, all blend films

exhibited contact angle values higher than 90°. Generally, the contact angle values in FG/CL blend films were within the range indispensable for commercial applications. It must be noted that materials with a non-absorbent surface, which are often used as hydrophobic references (93.9-100.2° for low-density polyethylene film and 91.5° for Plexiglas).[46] Etxabide et al.[47] reported that heat treated films, gelatine-lactose cross-linking by Maillard reaction decreased polar groups and thus, increased the hydrophobic character of films.

3.8. Spectral analysis

Fig.2 illustrates the FTIR spectra of the selected films in the range of 650-4000 cm^{-1}. The corresponding assignments of the absorption peaks are summarised in Table 4. As seen in the spectra, the typical bands of FG/CL (8:2) blend film and FG film were found in amide region. Those absorption bands in the range of 1800-600 cm^{-1} cover amide-I, amide-II and amide-III.[1] FG/CL (8:2) blend film and FG film exhibited the amide-I bands at the wavenumbers of 1642.2 and 1641.9 cm^{-1}, respectively. The shift of amide-I band to higher wavenumber in FG/CL (8:2) blend film represented significant decrease in molecular order due to conformational changes in film structure induced by the addition of CL.[2] This was primarily correlated with the decrease in tensile performance in FG/CL (8:2) blend film. The lower amplitude of amide-I band in FG/CL (8:2) blend film was attributed to the weaker intermolecular interaction between FG and CL reactive groups. The smaller band detected in CL film at the wavenumber of 1656.0 cm^{-1} was assigned to −OH stretching of water molecules strongly coupled with the amorphous structure of CL.[12] The amide-II band of FG/CL (8:2) blend film had slightly higher wavenumber (1550.6 cm^{-1}), compared to FG film (1550.3 cm^{-1}). Nevertheless, CL film (1561.8 cm^{-1}) showed the highest wavenumber at amide-II region, representing the vibrations of

N-H groups of indigenous protein components associated with CL.[48] The spectral differences among different films were attributed to intermolecular rearrangement, variable conformation and orientation of functional groups of polypeptide and polysaccharide chains. At amide-III region, CL incorporation led to slight shift to the lower wavenumber of FG/CL (8:2) blend film (1240.7 cm^{-1}), compared to FG film (1241.3 cm^{-1}). The dominant absorption bands in CL film representing the vibrations of C-O and C-OH groups were noticeable at the wavenumbers of 1203.8 and 1261.0 cm^{-1}, respectively. However, -CH and $-CH_2$ groups in CL film appeared at the wavenumber of 1375.5 and 1318.1 cm^{-1}, respectively. The major absorption bands that arose from asymmetric stretching vibrations of -OH groups of glycerol (plasticiser) coupled to $-CH_2$ of amino acid residues of FG film (1041.7 cm^{-1}) and FG/CL (8:2) blend film (1042.9 cm^{-1}); whereas, -OH groups of CL film (1039.9 cm^{-1}) interacted with the glycerol via hydrogen bonding.[49] The relatively broad bands in FG/CL (8:2) blend film and CL film at 1079.1 and 1073.0 cm^{-1} were assumed to the anhydro-glucose ring C-O stretching vibration[50,51] and at 926.1-925.9 cm^{-1} were associated with the C-H of residual carbons.[51] The smaller absorption band in FG/CL (8:2) blend film and CL film at 1161.6 cm^{-1} and 1158.3 cm^{-1} was assigned to the C-O-C linkage in the glycosidic structure.[50]

Moreover, CL film displayed the -OH stretching and C-H asymmetric stretching absorption bands at the wavenumber of 3331.7 cm^{-1} (broad) and 2921.3 cm^{-1} (medium), respectively. For amide-A band, FG/CL (8:2) blend film (3310.5 cm^{-1}) had the lower wavenumber, compared to FG film (3311.4 cm^{-1}). The shift to lower wavenumber at amide-A peak suggesting the conformational change in FG/CL (8:2) blend film. Typically, the decrease in vibrational wavenumber and broadening of the -OH and -NH vibration bands could be indicative of interaction between polymers in

the blend film.[52] It was postulated that the reactive group could undergo interaction to the lower extent in FG/CL (8:2) blend film, thereby resulting in more flexibility of the film. This was confirmed by the decreased TS and increased EAB of FG/CL (8:2) blend film in comparison with FG film. Additionally, FG/CL (8:2) blend film showed the lower wavenumber at amide-B peak (2933.8 cm^{-1}), compared to FG film (2937.8 cm^{-1}), suggesting the interaction of $–NH_3$ group with the functional groups of CL matix.[1] The shift to lower wavenumber at amide-B peak in the FG/CL (8:2) blend film indicated an increase in hydrogen bonding between two components in film matrix and likely led to changes in film properties. Thus, FTIR spectra reconfirmed the changes in molecular organisation and interaction in the film matrix of resulting FG/CL (8:2) blend film.

3.9. Differential scanning calorimetry (DSC)

DSC thermograms of 1st heating scan (A) and 2nd heating scan (B) of selected films are illustrated in Fig. 3 and their glass transition temperatures (T_g), melting transition temperatures (T_{max}) and enthalpies (ΔH) are shown in Table 5. Based on the 1st heating scan (from -30 to 200 °C), FG/CL (8:2) blend film exhibited higher endothermic temperature (T_{max}~89.7 °C) and enthalpy (ΔH~6.7 J/g), compared to FG film (T_{max}~71.5 °C; ΔH~0.9 J/g). T_{max} indicated the temperature causing a destruction of ordered or aggregated structure (crystalline phase) stabilised by various interactions.[2] Higher T_{max} of FG/CL (8:2) blend film, compared to FG film, indicated the formation of a three-dimensional (3D) network, in which zones of intermolecular microcrystalline junctions were formed. Moreover, the higher ΔH of FG/CL (8:2) blend film indicated that greater portion of ordered structure developed in the blend film.[4] Nevertheless, lower T_g was noted in FG/CL (8:2) blend film (30.2 °C), compared to FG film (34.6 °C), which was more likely associated with molecular

segmental motion of disordered (amorphous) structure. T_g is a physical parameter associated with the system mobility, which depends on molecular structure, intermolecular interaction and structural stiffness.[2] The physical change from the glassy to the rubbery state in amorphous materials stimulated by heat is referred as T_g. The amorphous regions of film produce elasticity and the crystalline regions contribute strength and rigidity.[53] Below T_g, films are rigid and brittle, whereas films become flexible and elastic above T_g.[54] Lower T_g of FG/CL (8:2) blend film was coincidental with the possible enhancement in the segmental flexibility of polymeric chains. Thus, CL inclusion softens the film matrix and consequently decreases the overall cohesion among the polymeric molecules as evidenced by the higher EAB. Additionally, water molecules associated with the CL structure tends to function as a plasticiser, thereby decreasing T_g. For FG film (1st heating scan), the endothermic peak was associated with the helix-coil transition and disruption of molecular ordered structure (turn or random coils).[55] During film formation, FG molecules undergo partial renaturation and subsequently stabilise the film structure.[4] For 2nd heating scan of FG/CL (8:2) blend film (from −30 to 300 °C), the thermogram displayed two separated endothermic peaks at the T_{max} of 121.6 °C (ΔH~1.5 J/g) and 247.7 °C (ΔH~13.5 J/g). This indicated that two different ordered structures coexisted in the FG/CL (8:2) blend film matrix; the lower T_{max} is dominated by FG/CL (amorphous and/or crystalline) and higher T_{max} is governed by CL (crystalline). Pertinently, FG and CL would remain intimately bonded in blend film with small phase domain dimensions via interfacial interaction as evidenced from FTIR result. In general, the interaction on molecular level between the amorphous phases of two biopolymers of sufficiently separated T_{max} leads to a single T_{max} for a blend film, intermediate between those of the homopolymers.[4] Therefore, endothermic peak at the T_{max} of

121.6 °C in the FG/CL (8:2) blend film could be due to significant shift of T_{max} towards intermediate position recognised as a sign of miscibility/stability or interfacial interaction. Moreover, the endothermic peak at the T_{max} of 247.7 °C observed in FG/CL (8:2) blend film suggested partial immiscibility between FG and CL molecules due to their distinct chemical structures. For FG film (2nd heating scan), no transition was observed since the bound water molecules acting as plasticiser might be evaporated during the 1st heating scan. As a consequence, the interaction between FG molecules was enhanced which led to the formation of more rigid film network. For CL film (1st heating scan), lower T_g (24.2 °C) was detected from the thermogram. Nevertheless, a broad peak arose at the T_{max} of 120.1 °C (ΔH~6.8 J/g) due to the disintegration of intra- and intermolecular cross-links stabilising the spindle-shaped pseudo-crystalline microfibrillar CL structure.[19] Higher T_{max} of CL film could be attributed to the swelling and melting of CL structure followed by disintegration of hydrophobic and hydrogen bonds.[19] The loss of cohesive structure integrity in CL could be explained by the fact that microfibrils dissociate at 60 °C in the first step as the hydrogen bonds were broken, but then eventually reassociate at higher temperatures due to hydrophobic interaction between CL molecules.[19] At lower temperatures, CL molecules are hydrated and there is little polymer-polymer interaction apart from simple entanglement. As the temperature increases, molecules absorb translational energy and gradually lose their hydrated water.[19] The anhydrous form of CL corresponds to a conformation based on single helix, whereas annealed (hydrate) CL is readily identified as the triple helix.[19] The single helix provides the strength to film stabilised by pseudo-crosslinks arising from hydrophobic associations. In CL film (2nd heating scan), two endothermic peaks appeared at 220.3 and 278.8 ºC, which were probably related to the complete decomposition of CL

structure caused by the breakdown of glycosidic bonds which generally held anhydro-D-glucose units together in linear chains.[56] However, higher T_g (80.2 ºC) was detected in CL film in 2nd heating scan. From the results, the increase in T_g or T_m could explain in part an increase in resistance and rigidity due to the evaporation of bound water molecules in 1st heating scan. As a consequence, the CL domains were more available for bonding among themselves. It was noted that CL is pseudo-crystalline polymer stabilised by strong intra- and intermolecular hydrogen bonds, and has a rigid amorphous phase due to its heterocyclic units.[48] Moreover, the higher value of ΔH (7.8-88.0 J/g) required to disrupt the film network possibly explained the increase in crystallinity behaviour of CL film. In general, extra energy (ΔH) was required by CL components to vibrate and breakdown the bonds out of the rigid molecular arrangement. Therefore, the addition of CL showed the pronounced impact on thermal properties (transition) of the resulting FG/CL (8:2) blend film due to the heterogeneous film matrix and stable molecular organisation bonded by various intermolecular interactions. Based on DSC results, it was postulated that the compatible FG/CL blend rendered the highly heat stable film matrix, which was stabilised by forming an ordered junction zones.

3.10. Thermo-gravimetric analysis (TGA)

TGA curves revealing thermal degradation behaviour of selected films are shown in Fig. 4. Their degradation temperatures (Td) and weight loss (Δw) are presented in Table 6. Four main weight loss stages were observed in FG/CL (8:2) blend film and CL film, but FG film exhibited three main weight loss stages. The first stage weight loss (Δw_1= 2.2 %) in FG/CL (8:2) blend film was observed at the onset temperature (Td$_1$) of 45.3 °C, mostly associated with the loss of free and bound water adsorbed in the film.[35] The first stage weight loss of FG (Δw_1= 5.0 %) and CL films

(Δw_1= 3.4 %) was observed over the onset temperature (Td$_1$) at 46.6 and 36.4 °C, respectively. Thus, lower first stage weight loss was observed in FG/CL (8:2) blend film and CL film, suggesting lower water desorption from film matrix linked by hydrogen bonds, compared to FG film. The second stage weight loss for FG/CL (8:2) blend film (Δw_2= 30.3 %) appeared at the onset temperature of 172.4 °C (Td$_2$), whilst FG and CL films showed weight loss (Δw_2= 13.1-56.2 %) over the onset temperature (Td$_2$) of 181.9-190.9 °C. This was most likely due to the degradation or decomposition of lower MW peptides, polysaccharide components, glycerol compounds along with evaporation of structurally bound water in the film network.[4] In general, FG/CL (8:2) blend film showed lower thermal resistance at second stage weight loss, compared to FG and CL film, as evidenced by the lower Td$_2$. For the third stage weight loss (Δw$_3$ = 10.2 %), Td$_3$ value of 272.9 °C was observed in FG/CL (8:2) blend film which was mostly associated with the degradation of the larger size or associated FG/CL fragments[8], whilst FG and CL films showed the Δw$_3$ of 7.5-55.1 % at the Td$_3$ of 289.7-318.9 °C. The results revealed that FG/CL (8:2) blend film showed lower thermal stability attributed to the partial interfacial interaction between D-glucosyl residues and amino acids, leading to the less heat resistance of the resulting blend film, compared to FG film.[35] For the fourth stage weight loss (Δw$_4$ = 6.2-22.9 %), Td$_4$ of 330.6 and 409.0 °C were obtained for FG/CL (8:2) blend film and CL film, respectively. Nevertheless, the fourth stage weight loss (Δw$_4$) disappeared in FG film. It was noted that the fourth stage weight loss might be associated with the loss of thermally stable components constituted in the film matrix and depolymerisation of macromolecular chains and the chemical bonds rupture. The residual masses (representing char content) at 600 °C were in the range of 26.5-34.1 % in all films. Based on char content, FG/CL (8:2) blend film showed enhanced heat

stability as evidenced by higher heat-stable mass residues (34.1 %, w/w). Slight difference in char content was most likely due to different formulation and types of components, their blend ratio, covalent and non-covalent interaction among the components in film matrix. Therefore, TGA curves showed clearly that addition of CL contributed to a substantial improvement in the thermal stability of the resulting FG/CL (8:2) blend film.

3.11. Morphology analysis

SEM micrographs of the surface (A) and cryo-fractured cross-section (B) of selected films are illustrated in Fig. 5. FG/CL (8:2) blend film had slightly irregular, protruded, heterogeneous and void/crack-free surface structure. The overlapping of FG and CL molecular segments mediated by covalent and non-covalent bonding enhanced the slight discontinuity and unevenness in the surface structure of FG/CL (8:2) blend film. In addition, slight phase separation along with larger aggregates or agglomerates on surface was noted in the matrix of FG/CL (8:2) blend film, indicating lower compatibility of the FG/CL blend. Those protruded zones in FG/CL (8:2) blend film were associated with the coexisting of different ordered junction zones, presumably formed in the film network. The protruded network of film structure led to increased thickness of resulting FG/CL (8:2) blend film (Table 1). It was further noted that CL was unevenly dispersed between the fibrillar zones of FG and showed lower interfacial adhesion with FG molecules. Nevertheless, non-porous, smooth and compact cross-section with minor heterogeneities was noticeable in FG/CL (8:2) blend film, indicating good structural integrity. FG film exhibited relatively smooth, continuous, compact and homogenous surface area, indicating that an ordered structure was formed without layering phenomenon. This was accompanied with the better mechanical and physical properties of FG film. FG molecular segments formed

the stronger film network with a great number of junction zones between the carbonyl and amide groups. As a result, the continuous strong matrix was developed. FG film also showed dense and uniform microstructure with minor heterogeneities in the cross-section which are typically found in brittle fracture. In CL film, the rough surface and looser network was observed which was in accordance with the poor mechanical properties, accompanied with higher WVP. These variations in microstructure of different films were caused by the different arrangements of biopolymers chains during film formation.[2,35] Thus, the microstructures of films were governed by molecular organisation in the film network, which depended on types of components, the interaction of components in film matrix as well as the blend ratio of components used for film preparation.

4. Conclusion

The properties of FG/CL blend films at alkaline pH were significantly affected by the addition of CL in the film formulation. Increased CL content in FG/CL blend films reduced the film strength (TS) and stiffness (E), but improved stretchability (EAB), thereby forming crack resistant film network. At pH 12, FG/CL blend yielded films with enhanced thickness, water resistance, contact angle and WVP. FG/CL blend films were significantly transparent and presented yellow colour development related to Malliard browning reaction, as well as, a higher UV absorption capacity which could be beneficial for prevention of lipid oxidation in foods. FG/CL (8:2) blend film was rougher than FG film, but no signs of phase separation between film components were observed on SEM micrographs. FTIR results suggested some structural modifications in FG/CL (8:2) matrix attributed to the interfacial interactions between FG/CL functional groups, which directly governed film properties. DSC evidenced the presence of distinctive domains corresponding to the aggregated

ordered structures in the FG/CL (8:2) blend film which led to the improved thermal stability, compared to FG film. FG/CL (8:2) blend film exhibited greater heat stability as evidenced by higher heat-stable mass residues. Based on the mechanical strength, adequate flexibility and stiffness, water resistance, UV absorption capacity and enhanced thermal stability, FG/CL (8:2) blend film has high potential to be used as packaging materials at industrial scale.

Acknowledgements

The authors would like to express their sincere thanks to the Institute of Nutrition (INMU), Mahidol University, Thailand for the research facilities.

References

1 M. Ahmad and S. Benjakul, *Food Hydrocoll.*, 2011, **25**, 381–388.

2 M. Ahmad, N. M. Hani, N. P. Nirmal, F. F. Fazial, N. F. Mohtar and S. R. Romli, *Prog. Org. Coat.*, 2015, **84**, 115–127.

3 M. Ahmad and S. Benjakul, *Process Biochem.*, 2011, **46**, 2021–2029.

4 M. S. Hoque, S. Benjakul, T. Prodpran and P. Songtipya, *Int. J. Biol. Macromol.*, 2011, **49**, 663–673.

5 R. A. de Carvalho and C. R. F. Grosso, *Food Hydrocoll.*, 2004, **18**, 717–726.

6 L. Mariniello, P. Di Pierro, C. Esposito, A. Sorrentino, P. Masi and R. Porta, *J. Biotechnol.*, 2003, **102**, 191–198.

7 B. Ouattara, L. T. Canh, C. Vachon, M. A. Mateescu and M. Lacroix, *Radiat. Phys. Chem.*, 2002, **63**, 821–825.

8 M. S. Hoque, S. Benjakul and T. Prodpran, *J. Food Eng.*, 2010, **96**, 66–73.

9 B. Li, J. F. Kennedy, Q. G. Jiang and B. J. Xie, *Food Res. Int.*, 2006, **39**, 544–549.

10 R. Tang, Y. Du, H. Zheng and L. Fan, *J. Appl. Polym. Sci.*, 2003, **88**, 1095–1099.

11 T. Karnezis, H. C. Fisher, G. M. Neumann, B. A. Stone and V. A. Stanisich, *J. Bacteriol.*, 2002, **184**, 4114–4123.

12 C. Wu, S. Peng, C. Wen, X. Wang, L. Fan, R. Deng and J. Pang, *Carbohydr. Polym.*, 2012, **89**, 497–503.

13 K. Nishinari and E. Doi, *Food Hydrocolloids: Structures, Properties, and Functions*, Springer Science & Business Media, 2012.

14 T. Funami, M. Funami, H. Yada and Y. Nakao, *Food Hydrocoll.*, 2000, **14**, 509–518.

15 K. Nishinari and H. Zhang, *Trends Food Sci. Technol.*, 2004, **15**, 305–312.

16 H. Zhang, K. Nishinari, M. A. K. Williams, T. J. Foster and I. T. Norton, *Int. J. Biol. Macromol.*, 2002, **30**, 7–16.

17 B. S. Kim, I. D. Jung, J. S. Kim, J. Lee, I. Y. Lee and K. B. Lee, *Biotechnol. Lett.*, 2000, **22**, 1127–1130.

18 S. Dumitriu, *Polysaccharides in Medicinal Applications*, CRC Press, 1996.

19 G. O. Phillips and P. A. Williams, *Handbook of Hydrocolloids*, Elsevier, 2009.

20 F. and D. Administration and O. of the F. R. (U.S.), *The Code of Federal Regulations of the United States of America*, U.S. Government Printing Office, 2001.

21 J. M. Lynch and D. M. Barbano, *J. AOAC Int.*, 1999, **82**, 1389–1398.

22 K. I. Iwata, S. H. Ishizaki, A. K. Handa and M. U. Tanaka, *Fish. Sci.*, 2000, **66**, 372–378.

23 Y. Shiku, P. Yuca Hamaguchi, S. Benjakul, W. Visessanguan and M. Tanaka, *Food Chem.*, 2004, **86**, 493–499.

24 A. Gennadios, A. Handa, G. W. Froning, C. L. Weller and M. A. Hanna, *J. Agric. Food Chem.*, 1998, **46**, 1297–1302.

25 A. Gennadios, C. l. Weller, M. a. Hanna and G. w. Froning, *J. Food Sci.*, 1996, **61**, 585–589.

26 A. Jongjareonrak, S. Benjakul, W. Visessanguan and M. Tanaka, *Food Hydrocoll.*, 2008, **22**, 449–458.

27 J. H. Han and J. D. Floros, *J. Plast. Film Sheeting*, 1997, **13**, 287–298.

28 P. Nuthong, S. Benjakul and T. Prodpran, *Int. J. Biol. Macromol.*, 2009, **44**, 143–148.

29 N. Limpan, T. Prodpran, S. Benjakul and S. Prasarpran, *J. Food Eng.*, 2010, **100**, 85–92.

30 J. P. Zheng, P. Li, Y. L. Ma and K. D. Yao, *J. Appl. Polym. Sci.*, 2002, **86**, 1189–1194.

31 B.-D. Kim, K. Na and H.-K. Choi, *Eur. J. Pharm. Sci.*, 2005, **24**, 199–205.

32 M. Dick, T. M. H. Costa, A. Gomaa, M. Subirade, A. de O. Rios and S. H. Flôres, *Carbohydr. Polym.*, 2015, **130**, 198–205.

33 T. Sivarooban, N. S. Hettiarachchy and M. G. Johnson, *Food Res. Int.*, 2008, **41**, 781–785.

34 Y. A. Arfat, S. Benjakul, T. Prodpran and K. Osako, *Food Hydrocoll.*, 2014, **39**, 58–67.

35 M. Ahmad, S. Benjakul, T. Prodpran and T. W. Agustini, *Food Hydrocoll.*, 2012, **28**, 189–199.

36 B. W. S. Souza, M. A. Cerqueira, J. A. Teixeira and A. A. Vicente, *Food Eng. Rev.*, 2010, **2**, 244–255.

37 H. J. Park and M. S. Chinnan, *J. Food Eng.*, 1995, **25**, 497–507.

38 M. Maizura, A. Fazilah, M. H. Norziah and A. A. Karim, *J. Food Sci.*, 2007, **72**, C324–330.

39 S. Tunc, H. Angellier, Y. Cahyana, P. Chalier, N. Gontard and E. Gastaldi, *J. Membr. Sci.*, 2007, **289**, 159–168.

40 J. W. Rhim, A. Gennadios, A. Handa, C. L. Weller and M. A. Hanna, *J. Agric. Food Chem.*, 2000, **48**, 4937–4941.

41 S. Mathew, M. Brahmakumar and T. E. Abraham, *Biopolymers*, 2006, **82**, 176–187.

42 T. Prodpran, S. Benjakul and A. Artharn, *Int. J. Biol. Macromol.*, 2007, **41**, 605–614.

43 M. Pereda, A. G. Ponce, N. E. Marcovich, R. A. Ruseckaite and J. F. Martucci, *Food Hydrocoll.*, 2011, **25**, 1372–1381.

44 P. Guerrero, Z. A. Nur Hanani, J. P. Kerry and K. de la Caba, *J. Food Eng.*, 2011, **107**, 41–49.

45 Y. Yuan and T. R. Lee, in *Surface Science Techniques*, eds. G. Bracco and B. Holst, Springer Berlin Heidelberg, 2013, pp. 3–34.

46 S. Galus and J. Kadzińska, *Food Hydrocoll.*, 2016, **52**, 78–86.

47 A. Etxabide, J. Uranga, P. Guerrero and K. de la Caba, *LWT - Food Sci. Technol.*, 2015, **63**, 315–321.

48 Y. Sun, Y. Liu, Y. Li, M. Lv, P. Li, H. Xu and L. Wang, *Carbohydr. Polym.*, 2011, **84**, 952–959.

49 I. Leceta, P. Guerrero, I. Ibarburu, M. T. Dueñas and K. de la Caba, *J. Food Eng.*, 2013, **116**, 889–899.

50 M. Poletto, V. Pistor and A. J., in *Cellulose - Fundamental Aspects*, ed. T. G. M. Van De Ven, InTech, 2013.

51 J. M. Fang, P. A. Fowler, J. Tomkinson and C. A. S. Hill, *Carbohydr. Polym.*, 2002, **47**, 245–252.

52 B. B. Doyle, E. G. Bendit and E. R. Blout, *Biopolymers*, 1975, **14**, 937–957.

53 Y. Freile-Pelegrín, T. Madera-Santana, D. Robledo, L. Veleva, P. Quintana and J. A. Azamar, *Polym. Degrad. Stab.*, 2007, **92**, 244–252.

54 M. Ghasemlou, F. Khodaiyan and A. Oromiehie, *Carbohydr. Polym.*, 2011, **84**, 477–483.

55 M. S. Rahman, G. S. Al-Saidi and N. Guizani, *Food Chem.*, 2008, **108**, 472–481.

56 F. A. López, A. L. R. Mercê, F. J. Alguacil and A. López-Delgado, *J. Therm. Anal. Calorim.*, 2007, **91**, 633–639.

Figure Legends:

Fig.1. Water contact angle of blend films prepared at different FG/CL ratios (pH 12).

Fig.2. FTIR spectra of films from FG, CL and FG/CL (8:2) blend.

Fig.3. DSC thermograms of 1st heating scan (A) and 2nd heating scan (B) of films from FG, CL and FG/CL (8:2) blend.

Fig.4. TGA and DTG curves of films from FG, CL and FG/CL (8:2) blend.

Fig.5. SEM micrographs of surface (A) and cryo-fractured cross-section (B) of films from FG, CL and FG/CL (8:2) blend.

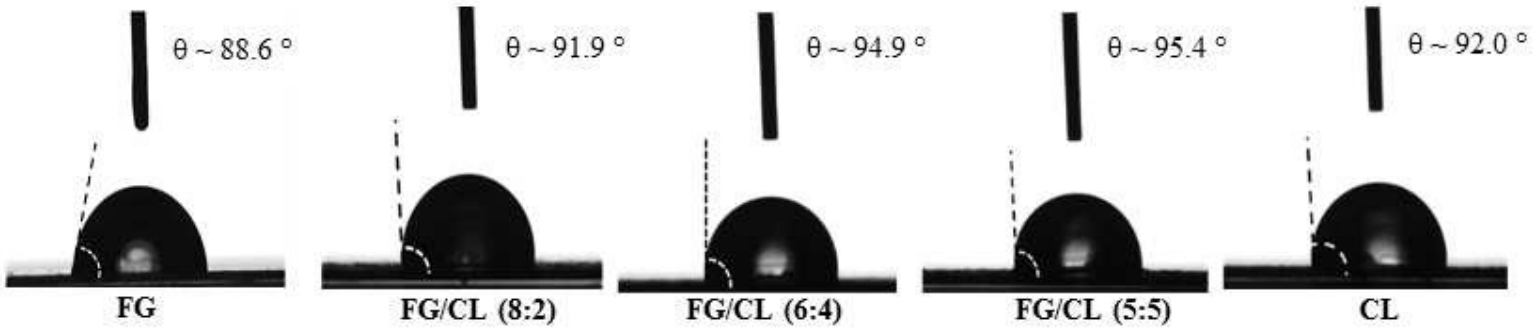

Fig. 1.

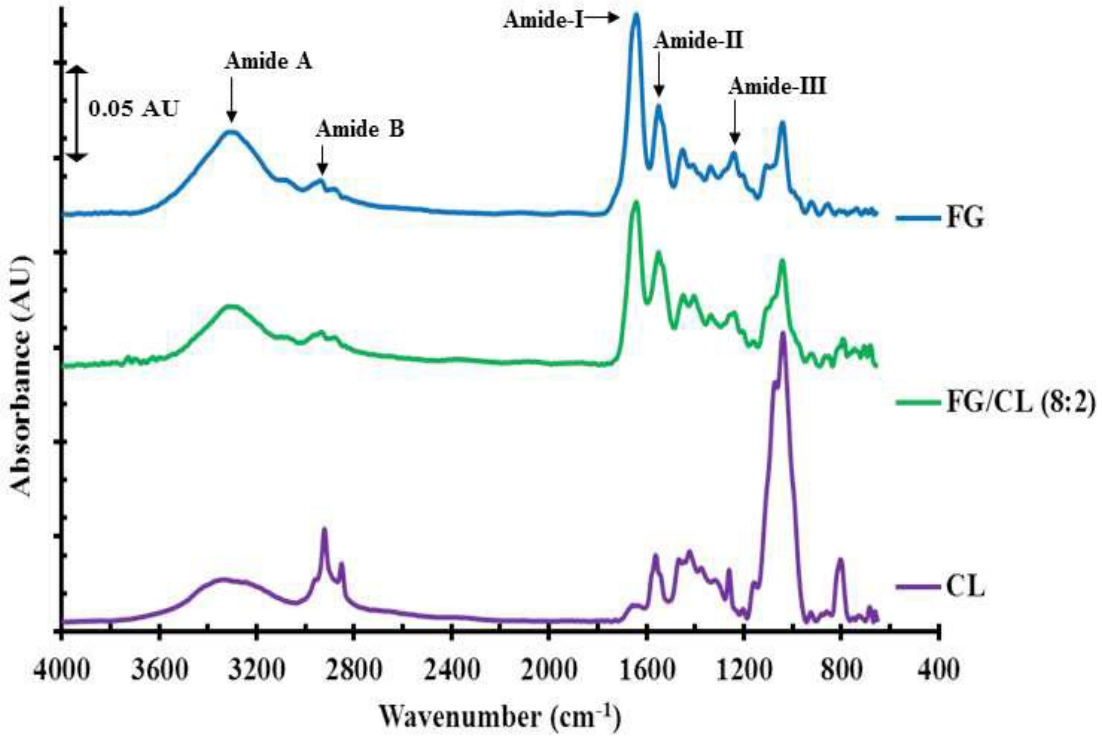

Fig. 2

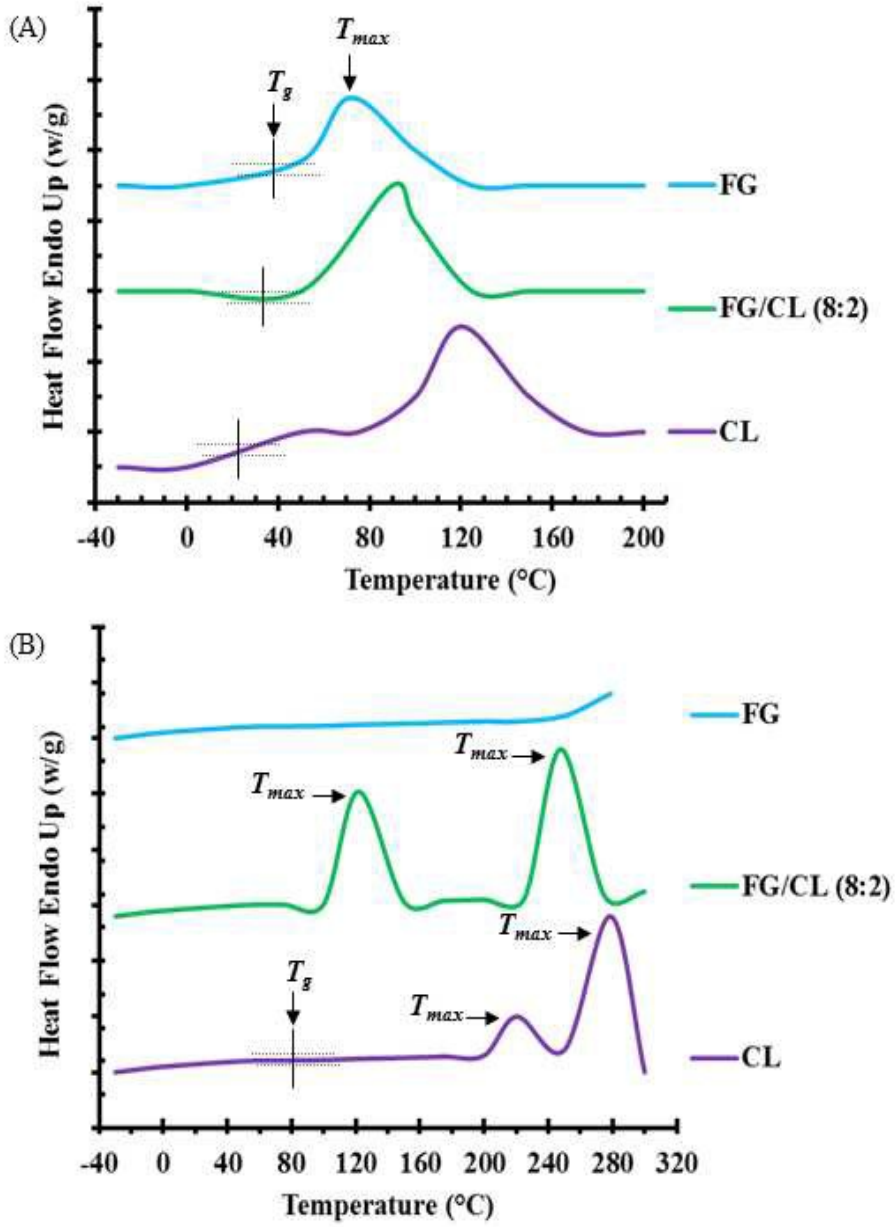

Fig. 3.

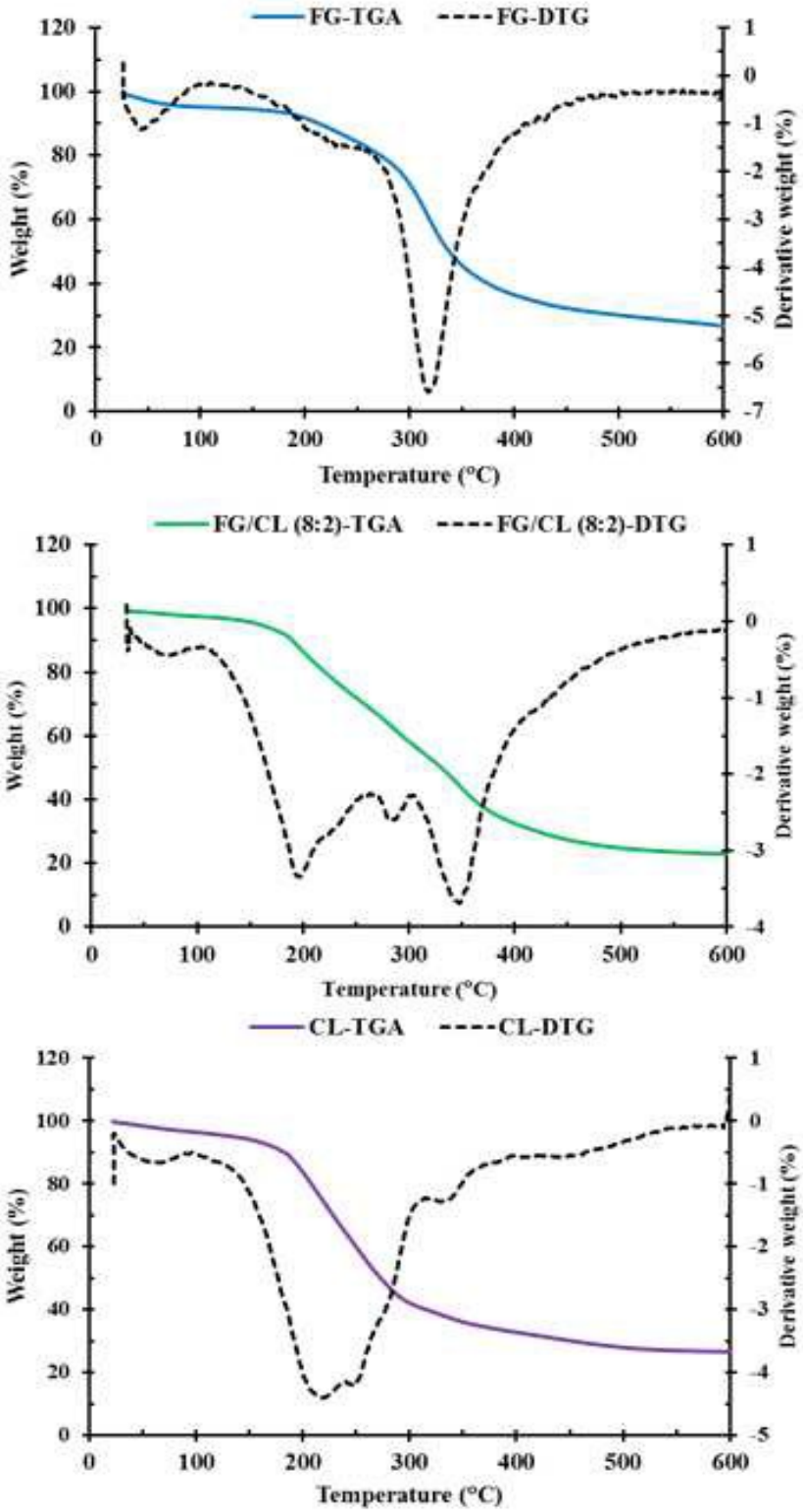

Fig. 4.

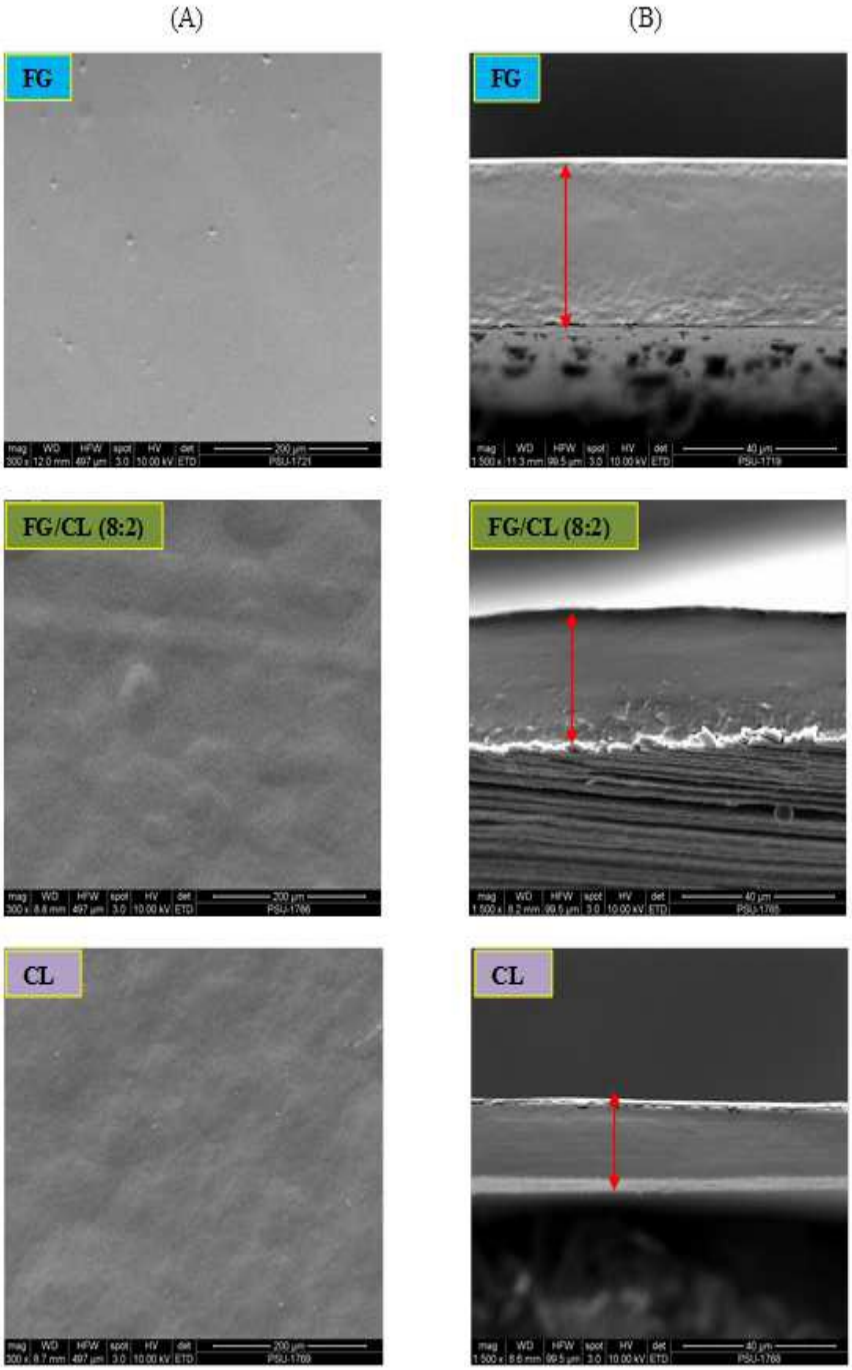

Fig. 5.

Table 1. Tensile strength (TS), Young's Modulus (E), elongation at break (EAB), water vapour permeability (WVP) and thickness of blend films prepared at different FG/CL ratios

Film Samples	pH	TS (MPa)	E (MPa)	EAB (%)	WVP× (10^{-10}gs^{-1}m^{-1}Pa^{-1})	Thickness (μm)
FG/CL (10:0)	7	33.2±1.8A	753.9±3.3A	9.6±0.0B	2.8±0.0B	20.0±3.0A
FG/CL (10:0)	12	25.3±4.1aB	685.5±3.0aB	14.7±3.3cA	3.0±0.0bA	20.0±3.0dA
FG/CL (8:2)	12	20.5±1.3b	496.7±2.0b	21.8±1.8b	4.7±0.6a	27.0±1.0c
FG/CL (6:4)	12	8.5±0.9cd	177.8±1.1d	38.3±3.2a	5.9±0.8a	35.0±2.0b
FG/CL (5:5)	12	6.7±1.5d	153.8±1.0e	41.3±4.8a	7.8±0.8a	46.0±2.0a
FG/CL (0:10)	12	9.6±1.3c	235.3±1.9c	15.3±3.6c	6.0±0.8a	32.0±4.0b

Values are given as mean ± SD (n = 3).
FG/CL (Fish gelatine/Curdlan)
Different letters (a, b, c, d, e) in the same column indicate significant differences (P<0.05).
Different capital letters in the same column indicate the significant differences between FG film prepared at pH 7 and pH 12 (P<0.05).

Table 2. Colour properties, solubility and moisture content of blend films prepared at different FG/CL ratios

Film Samples	pH	Colour				Solubility (%)	Moisture (%)
		L^*	a^*	b^*	ΔE^*		
FG/CL (10:0)	7	90.0±0.2A	-1.2±0.0A	0.8±0.1A	2.8±0.5A	94.9±0.2A	15.1±0.9A
FG/CL (10:0)	12	90.0±0.3bA	-1.2±0.0aA	0.8±0.1cA	2.8±0.3abA	94.4±0.5aA	15.3±0.9Ad
FG/CL (8:2)	12	91.2±0.2a	-1.6±0.0b	2.0±0.1b	2.2±0.2b	63.9±0.8d	19.5±0.82c
FG/CL (6:4)	12	90.7±0.2ab	-1.7±0.0b	2.5±0.2b	2.8±0.3ab	67.9±0.8b	22.3±0.3b
FG/CL (5:5)	12	90.3±0.8b	-1.7±0.0b	3.3±0.8a	3.8±1.2a	65.4±0.9c	25.1±0.2a
FG/CL (0:10)	12	90.5±0.2ab	-13±0.1a	1.4±0.3b	2.6±0.3ab	33.5±0.5e	20.1±0.3c

Values are given as mean ± SD (n = 3).
FG/CL (Fish gelatine/Curdlan)
Different letters (a, b, c, d, e) in the same column indicate significant differences (P<0.05).
Different capital letters in the same column indicate the significant differences between FG film prepared at pH 7 and pH 12 (P<0.05).

Table 3. Light transmittance (%) and transparency values of blend films prepared at different FG/CL ratios

Film Samples	pH	Wavelength (nm)								Transparency values
		200	280	350	400	500	600	700	800	
FG/CL (10:0)	7	0.0	48.6	80.0	82.6	84.0	**84.7**	86.9	87.2	3.7±0.0A
FG/CL (10:0)	12	0.0	50.0	81.8	84.1	86.3	**87.4**	88.2	88.6	3.6±0.0aB
FG/CL (8:2)	12	0.0	31.4	48.3	51.1	54.6	**56.5**	57.7	58.8	3.3±0.0c
FG/CL (6:4)	12	-0.0	28.5	58.6	65.5	72.7	**76.5**	79.1	81.0	3.3±0.0b
FG/CL (5:5)	12	0.0	20.1	41.4	46.9	53.7	**57.9**	61.0	63.6	3.0±0.0d
FG/CL (0:10)	12	1.4	55.1	72.5	77.0	81.3	**83.5**	84.9	86.0	3.4±0.0b

Values are given as mean ± SD (n = 3).
FG/CL (Fish gelatine/Curdlan)
Different letters (a, b, c, d, e) in the same column indicate significant differences (P<0.05).
Different capital letters in the same column indicate the significant differences between FG film prepared at pH 7 and pH 12 (P<0.05).

Table 4. Assignments of the bands in the FTIR spectra of selected films

Assignments	Wavenumber (cm^{-1})		
	FG	**FG/CL (8:2)**	**CL**
-NH stretching vibration, coupled with hydrogen bonding	3311.4	3310.5	-
-CH asymmetric stretching	2881.9	2880.4	2921.3
			2851.2
			1375.5
$-CH_2$ asymmetric stretching	2937.8	2933.8	
$-CH_2$ asymmetric bending	1451.8	1448.8	1466.5
	1410.0	1405.2	1423.4
C=O stretching/hydrogen bonding coupled with the CN stretch, CCN deformation and in-plane NH	1641.9	1642.2	
N-H bending vibration/ C-N stretching vibrations	1550.3	1550.6	1561.8
C-N stretching/ in-plane N-H bending/CH_2 stretching vibrations	1241.3	1240.7	
O-H stretching of glycerol molecules	1041.7	1042.9	
O-H stretching of water molecules			1656.0
O-H stretching vibrations			3331.7
O-CH skeletal vibrations		1336.1	1318.1
C-O stretching vibration (anhydro-glucose ring)		1079.1	1073.0
C-O stretching vibration		1206.2	1203.8
C-O stretching at C^2		1161.6	1158.3
C-O stretching at C^1 and C^3			1039.9
C-OH stretching vibration		1240.7	1261.0
C-O-C asymmetric stretching vibration		1161.6	1158.3
C-C skeletal vibrations	737.3	746.9	743.4
	855.1	865.7	860.4
	924.2	926.1	925.9

Table 5. Glass transition temperature (T_g), endothermic transition temperature (T_{max}), transition enthalpy (ΔH) of selected film samples

Film Samples	pH	1st heating scan			2nd heating scan			
		T_g (°C)	T_{max}(°C)	ΔH (J/g)	T_g (°C)	T_{max}(°C)		ΔH (J/g)
FG/CL (10:0)	12	34.6	71.5	0.9	-	-		-
FG/CL (8:2)	12	30.2	89.7	6.7	-	1st Peak	121.6	1.5
						2nd Peak	247.7	13.5
FG/CL (0:10)	12	24.2	120.1	6.8	80.2	1st Peak	220.3	7.8
						2nd Peak	278.8	88.0

Values are given as mean ± SD (n = 3).
FG/CL (Fish gelatine/Curdlan)

Table 6. Thermal degradation temperature (*T*d, °C) and weight loss (*Δw*, %) of selected film samples

Film samples	pH	Δ_1		Δ_2		Δ_3		Δ_4		Residue (%)
		$Td_{1\ onset}$ (°C)	Δw_1 (%)	$Td_{2\ onset}$ (°C)	Δw_2 (%)	$Td_{3\ onset}$ (°C)	Δw_3 (%)	$Td_{4\ onset}$ (°C)	Δw_4 (%)	
FG/CL (10:0)	12	46.6	5.0	190.9	13.1	289.7	55.1	-	-	26.6
FG/CL (8:2)	12	45.3	2.2	172.4	30.3	272.9	10.2	330.6	22.9	34.1
FG/CL (0:10)	12	36.4	3.4	181.9	56.2	318.9	7.5	409.0	6.2	26.5

Δ_1 , Δ_2, Δ_3 and Δ_4 denote the first, second, third and fourth stage weight loss, respectively, of film during TGA heating scan.

FG/CL (Fish gelatine/Curdlan)

Graphical Abstract

Blend film based on fish gelatine/curdlan for packaging applications: Spectral, microstructural and thermal characteristics

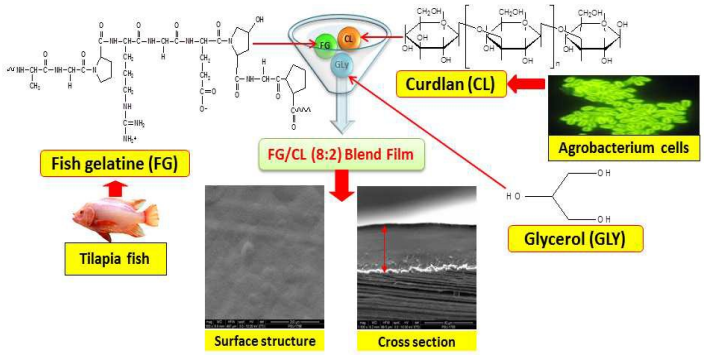

Novel biodegradable and thermostable FG/CL (8:2) blend film was fabricated and characterised for packaging applications.